AN INVESTIGATION OF WAVE SHELTERING BY ISLANDS

BY

S. V. Hsiao[1], J. F. Vesecky[2], and O. H. Shemdin[1]

SUMMARY

The West Coast Experiment, a meso-scale oceanographic experiment, was conducted from February to April, 1977, off the coast of Southern California. The wave data measured by an air-borne synthetic aperture radar (SAR) and a shore-based high frequency (HF) radar on March 25, 1977, are used to study the sheltering effect of islands on waves propagating towards shore. The comparisons between wave directional spectra offshore, in the vicinity of islands, and nearshore show that islands play a significant role in determining the near shore wave climate. The data show clearly the "shadow" and "window" effects. An investigation of waves coming out of the "shadow" region indicates that nonlinear wave-wave energy transfer is the likely mechanism responsible for producing such waves.

I. Introduction

The study of waves around islands was one of the objectives of the West Coast Experiment (Shemdin, 1980) conducted from February to April, 1977 off the coast of Southern California. To this objective, waves were measured by synthetic aperture radar (SAR), high frequency (HF) radar, wave rider buoy, and pressure sensor array. The use of radar made it possible to obtain wave measurements over a large area in a short period under various weather conditions. The Jet Propulsion Laboratory (JPL) L-band SAR was flown aboard a NASA CV-990 airplane at 8500m altitude and 240 m/sec speed. The flight paths relevant to this study are shown in Figure 1. The HF radar was operated from the coast south of San Clemente, California. This radar measured the energy of waves at 77m wave length (corresponding to .142 Hz frequency in deep water) moving directly toward or away from the radar site. The extent of HF radar observations is also shown in Figure 1. Wave measurements on March 25, 1977, are used in this study because all the above mentioned sensors were operating on that day and the dominent wave length match the wavelength HF radar observed. The wave spectra measured by pressure sensor array and wave rider buoy show that the primary peak at Torrey Pines and the secondary peak northwest of San Clemente Island are both near the wave frequency (.142 Hz) HF radar observed. The effects of islands on the directional properties of waves at this frequency are examined in this paper. The mechanisms which could generate waves coming out of the shadow of San Clemente Island are then discussed.

---

[1]Jet Propulsion Laboratory, California Institute of Technology

[2]Stanford Center for Radar Astronomy, Stanford University

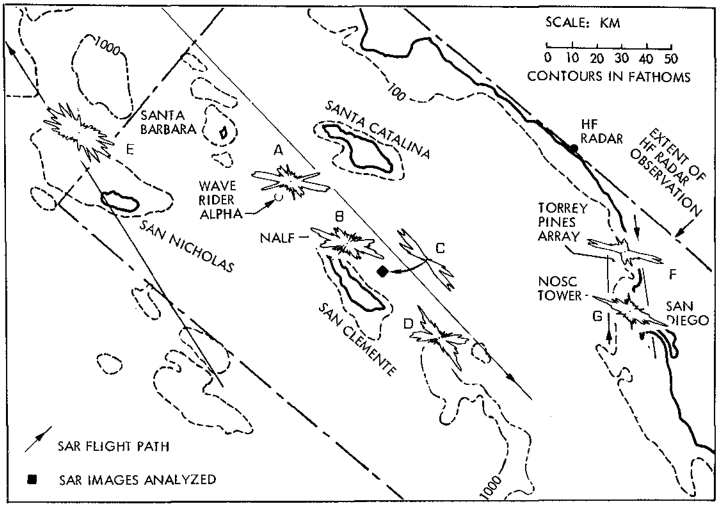

FIGURE 1. The West Coast Experiment area. Also shown are the normalized directional distributions of 80m waves measured by the L-band SAR on March 25, 1977, and the extent of HF radar observation.

II. THE SYNTHETIC APERATURE RADAR OBSERVATIONS

The synthetic aperture radar is an airborne or spaceborne microwave active sensing system. It uses its own power to transmit electromagnetic waves as the illumination. Therefore it has all weather and day/night capability. The SAR takes the advantage of the motion of aircraft or spacecraft to form a long "synthetic" antenna thus increases its azimuth (along track) resolution of the images. For the detail of the SAR system, see Brown and Porcello (1969).

The ability of SAR to image the ocean surface wave patterns have been deomonstrated by Brown et al. (1973), Elachi (1976), and others. But the systematic measurements and comparisons of SAR and conventional surface wave instruments were not done until the Marineland Experiment (Shemdin, 1980). The Marineland Experiment was conducted during December, 1975, off the Florida Atlantic coast. The simultaneous wave measurements by SAR, pitch-and-roll buoy, and pressure sensor were compared (Shemdin et al., 1978; Hsiao, 1978; and McLeish et al., 1980). It was found that the dominent wave frequencies and parameterized wave directional distributions can be detected by SAR accurately (see Table 1). The comparisons of wave measurements by SAR, pressure sensor array, CERC coastal radar, and aerial photos during the West Coast Experiment (Mattie et al., 1980) show similar results (see Figure 2). Furthermore, the wave directional measurements obtained during the West Coast Experiment by SAR and a pressure sensor array were compared by Pawka et al. (1980). The results show generally favorable agreement at the primary mode of the normalized directional distribution. A comparison for 6.9 sec waves is shown in Figure 3. Although the SAR imaging mechanism of ocean surface waves is not yet fully understood, these SAR-ground truth comparisons show that the SAR can provide useful information on the dominant wave frequency and the wave directional distributions

The Jet Propulsion Laboratory (JPL) L-band SAR operates at a frequency of 1.2 GHz corresponding to a wave length of 25 cm (see Brown et al., 1976). The signals returned from the ocean surface were recorded on the signal film by optical recorders on board the airplane. The signal film was then optically processed to form the raw image of the ocean surface. The resolution of this system is estimated to be 25m. The image was further digitized and geometrically corrected for the slant range distortion. Finally two-dimensional fast Fourier transforms were taken at selected locations to obtain two-dimensional wave number spectra. Examples of a geometrically corrected image and its 2-d FFT are shown in Figure 4. This image was taken near Torrey Pines, California at 1154 PST, March 25, 1977.

The directional distributions at 80m wavelength, which is the spectral peak on March 25, 1977, were plotted by tracing along circles centered at the origin with the radius $k=2\pi/80m$ on the 2-d spectra. The normalized directional distributions under this study are shown in Figure 1 for a few carefully selected locations. The 180° ambiguity can be resolved by assuming that all waves were propagating shoreward.

TABLE 1. SAR - SURFACE TRUTH COMPARISONS, MARINELAND EXPERIMENT (afte Hsiao, 1978)

(a) Comparisons of Peak Frequency and Peak Direction

	SAR	P-R BUOY	PRESSURE GAUGE
OBSERVED PEAK WAVE LENGTH (M)	80.4		
WAVE LENGTH CORRECTION (M)	4.6		
PEAK WAVE LENGTH (M)	85.0		
PEAK FREQUENCY (Hz)	0.122	0.125	0.117
OBSERVED PEAK DIRECTION (DEGREES TOWARD)	282		
DIRECTION CORRECTION (SAR)	-6		
DIRECTION CORRECTION (REFRACTION)	-5		
PEAK DIRECTION	271	270	

(b) Comparisons of Directional Distribution Parameters

	SAR	P-R	SAR	P-R	SAR	P-R	
WAVE LENGTH (M)	85.0		62.2		40.2		
FREQUENCY (Hz)	0.122	0.125	0.151	0.156	0.195	0.188	0.203
PEAK DIRECTION (DEGREES TOWARD)	271	270	270	267	266	268	275
P (1ST HARMONIC)	21	21	14	10	12	10	7
P (2ND HARMONIC)	19	28	14	11	13	11	8

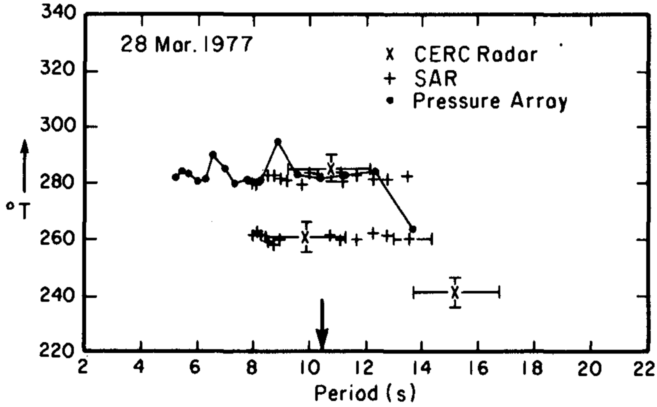

FIGURE 2. Comparisons of wave direction measurements among SAR CERC Coastal radar, and pressure array, (After Mattie et al., 1980)

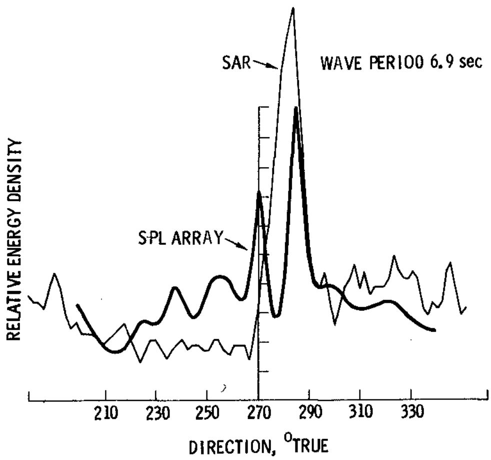

FIGURE 3. Comparison of directional distribution of 6.9 sec waves estimated by SAR and pressure sensor array, March 25, 1977, near Torrey Pines, California (After Pawka et al., 1980)

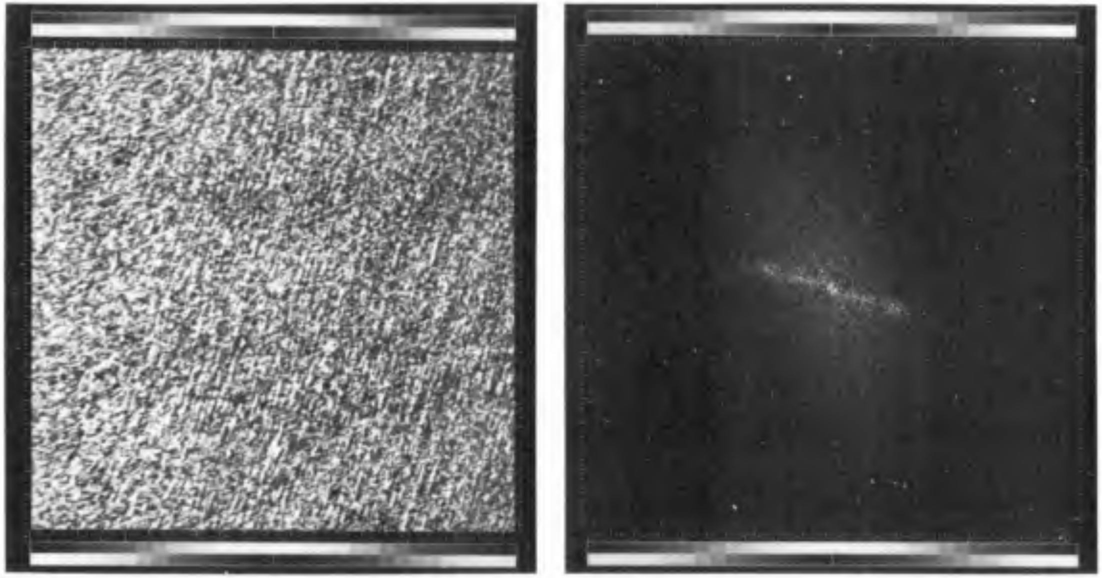

(a) (b)

FIGURE 4. (a) Geometric corrected SAR image near Torrey Pines, California, March 25, 1977. Each small division is approximately 54m.

(b) 2 - d FFT of (a), the wave number scale in each small division is is 0.0057 m^{-1}.

In Figure 1, the directional distribution at E, northwest of San Nicholas Island, is relatively broad. There is no island sheltering effect on this distribution. The directional distributions at A and B show the shadow effects of Santa Barbara and San Nicholas Islands. The directional distributions at C and D show significant shadow effects of San Clemente Islands. Comparing the distributions at C and E, only the waves parallel to San Clemente Island are detected at C, the rest of the waves are blocked by the Island. The distribution at D also shows the wave components detected at C. In addition it shows the wave components passing by the southern tip of San Clemente Island. The gap between the two groups of waves shows the shadow of San Clemente Island clearly. At F and G, the directional peaks both point to the window between San Clemente and Santa Catalina Islands, thus clearly showing the line of penetration of wave energy. These measurements indicate that a broad directional wave distribution offshore can be significantly different behind the islands. The distributions become narrow and multi-peaked because of the shadow effects. The distributions nearshore have peak directions aligned with the window between islands.

III. THE HIGH FREQUENCY RADAR OBSERVATIONS

The HF radar was operated in a synthetic aperature mode with a frequency of 1.9 MHz. This radar measures, by the first-order Bragg resonance, the energy of waves having a wavelength (77m) equal to one half the radar wavelength (154m) moving radially toward or away from the radar (Teague et al., 1975). This ocean wavelength corresponds to the spectral peak of waves measured on March 25, 1977. It has been shown experimentally that the HF radar echo energy is proportional to the resonant ocean wave energy (Teague et al., 1975). During this experiment, the 1 MW peak power LORAN-A transmitter at San Mateo Point, California was used as the signal source. The receiving antenna was synthesized by driving a van at a fixed speed along nearly straight stretches of interstate highway 5. This radar system has an azimuth resolution of 4° and a range resolution of 5 km.

The result of HF radar observation on March 25, 1977, is shown in Figure 5. The 5 dB contours show relative wave energy of 77m wavelength which moves radially toward the radar site. The shadow region of San Clemente Island and the window between Santa Cataline and San Clemente Islands are clearly shown in this Figure.

IV. WAVE TRANSFORMATION MECHANISMS IN THE VICINITY OF ISLANDS

In order to interpret the significance of the results, in Figure 6 the wave energy is plotted versus the distance from radar for two radial lines. One passes through the center of San Clemente Island and the other passes through the center of the window between San Clemente and Santa Catalina Islands. The energy level shown is the average of 10° azimuth angles and 10 km range distances. The steep drop of wave energy at San Clemente Island again shows the shadow effects. After passing San Clemente Island both curves of wave energy show approximately linear increases of the same slope in dB scale, or exponential increase in linear scale.

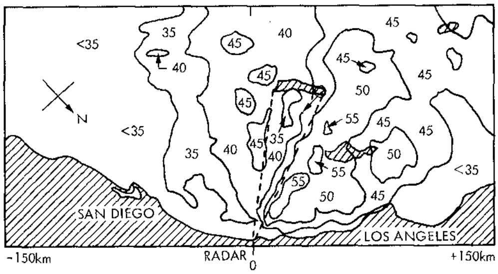

FIGURE 5. HF radar observations of 77m waves approaching the radar site. The contours show relative wave energy on dB scale.

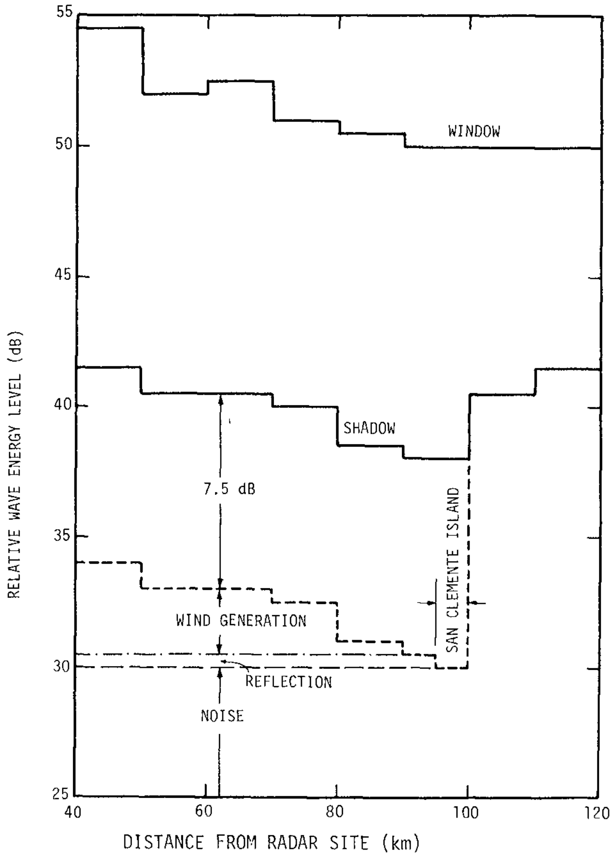

FIGURE 6. Relative wave energy level of 77m waves approaching HF radar site, averaged over 10° azimuth angles and 10 km range distances.

These results suggest that there must be local wave generation. The wind measurements over the West Coast Experiment area show the wind speed to be too small to contribute to the generation of 77m waves during this period. However, no reliable measurement were recorded in the wave generation area.

Despite the reduced level of wave energy behind San Clemente Island, the energy level is still significantly higher than the noise level. The contributions to the measured energy in the shadow of the Island from the waves passing by the northern and southern tips of the Island through the antenna side lobes are considered. The energy average is taken over 10° azimuth along the center of the shadow which is 19° wide. The effect of antenna side lobes is found to be negligible in this average region. The question regarding the mechanism by which waves gain energy in the shadow arises.

Since the water depth increases abruptly near San Clemente Island, the refraction of 77m waves is limited to narrow regions at the northern and southern tips of the Island. The same is true for the diffraction of waves. Thus the waves observed behind the Island in the center of the shadow region cannot be explained by either refraction or diffraction. The HF radar also measures the waves going away from the radar. The energy of such outgoing waves near San Clemente Island was $\sim$ 25 dB. The reflection of these waves by San Clemente Island has some contributions to the observed energy in the shadow region. But even assuming 100% reflection the reflected wave energy is too weak to account for the observed energy, (see Figure 6). By adding the wind generated energy estimated from Figure 6 to the energy level, there is still 7.5 dB difference to be explained.

The SAR data show that behind San Clemente Island there are waves propagating parallel to the direction of the Island. The transfer of energy from these waves to those toward the radar site through nonlinear interaction is suspected to be the source of the observed waves. The computation of the nonlinear energy transfer involves the evaluation of the Boltzmann integral describing by Hasselmann (1963). It is beyond the scope of this paper and is being pursued seperately.

V. CONCLUSION

The use of SAR and HF radar made it possible to obtain an overall view of wave conditions off the coast of Southern California. The study of waves at about 80m wavelengh on March 25, 1977, gives the following conclusions:

1. The shadow of San Clemente Island and the window between Santa Catalina and San Clemente Islands significantly modify the deep water wave spectrum as it propagates towards the coast.

2. The nonlinear transfer is the most likely source of the observed wave energy moving out of the shadow of San Clemente Island.

3. Remote sensing by SAR and HF radar provides useful information for the study of waves around islands.

ACKNOWLEDGEMENTS

The Jet Propulsion Laboratory contributions were supported by the National Aeronautic and Space Administration under contract NAS 7-100. The Stanford University contribution was supported by the Office of Naval Research under contract N-00017-75-C-0356.

REFERENCES

Brown, Jr., W. E., C. Elachi, and T. W. Thompson, (1976), Radar imaging of ocean surface patterns, J. Geophy. Res., 81, 2657-2667.

Brown, W. H. and L. Porcello, (1969) An introduction to synthetic aperture radar, IEEE Spectrum, 52-60.

Elachi, C., (1976) Wave patterns across the North Atlantic on September 28, 1974 from airborne radar imagery, J. Geophy. Res., 81, 26.

Hasselmann, K., (1963) On the nonlinear energy transfer in a gravity-wave spectrum. 3: Computation of the energy flux and the swell-sea interaction for a Neumann spectrum, J. Fluid Mech., 15, 385-398.

Hsiao, S. V., (1978) The comparison between the synthetic aperture radar imageries and the surface truth of ocean waves, Oceans '78, Marine Tech. Soc., Washington, D.C., 385-389.

Mattie, M. G., D. D. Evans and S. V. Hsiao, (1980) Wave direction measured by four different systems, submitted to Proc. ASCE WW.

McLeish, W., D. Ross, R. A. Shuchman, P. G. Teleki, S. V. Hsiao, O. H. Shemdin, W. E. Brown, Jr., (1980) Synthetic-aperture radar imaging of ocean waves: Comparison with wave measurements, J. Geophy. Res., in press.

Pawka, S. S., S. V. Hsiao, O. H. Shemdin, and D. L. Inman, (1980) Comparison between wave directional spectra from SAR and pressure sensor arrays, J. Geophy. Res., in press.

Shemdin, O. H., (1980) The Marineland Experiment: An Overview, EOS, in press.

Shemdin, O. H., (1980) The West Coast Experiment: An Overview, EOS, in press.

Shemdin, O. H., W. E. Brown, Jr., F. G. Staudhammer, R. Shuchman, R. Rawson, J. Zelenka, D. B. Ross, W. McLeish, and R. A. Berles, (1978) Comparison of in-situ and remotely sensed ocean waves off Marineland, Florida, Boundary-Layer Meteorology, 13, 193-202.

Teague, C. C., G. L. Tyler and R. H. Stewart, (1975) The radar cross-section of the sea at 1.95 MHz; comparison of in-situ and radar determination, Radio Science, 10, 847-852.